Electronic Journal of Biotechnology 67 (2024) 1–12

Contents lists available at ScienceDirect

Electronic Journal of Biotechnology

journal homepage: www.elsevier.com/locate/ejbt

Research article

SNORD3A acts as a potential prognostic and therapeutic biomarker in gastric cancer ☆

Qi Wang [a,*], Yifan Li [a], Xiaoqiang Niu [b], Chengjiang Zhang [a], Jun Zhang [a], Jiaqing Cao [b,*], Lidong Wu [a]

[a] Department of Emergency, The Second Affiliated Hospital of Nanchang University, Nanchang, Jiangxi, PR China
[b] Department of General Surgery, The Second Affiliated Hospital of Nanchang University, Nanchang, Jiangxi, PR China

GRAPHICAL ABSTRACT

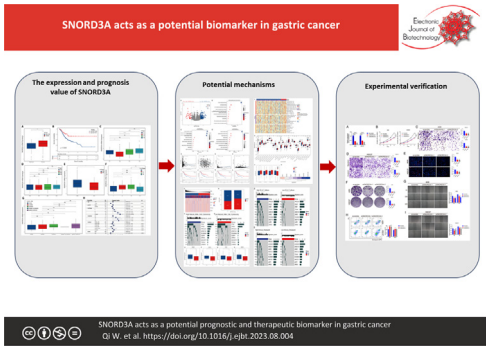

ARTICLE INFO

Article history:
Received 21 May 2023
Accepted 30 August 2023
Available online 27 October 2023
Peer review under responsibility of Pontificia Universidad Católica de Valparaíso

Keywords:
Gastric cancer
Gastric cancer invasiveness
Gastric cancer migration
Gastric cancer proliferation
GO-KEGG analysis
Kaplan-Meier curves
Prognostic biomarker
SNORD3A
Therapeutic biomarker

ABSTRACT

Background: Although SNORD3A has been implicated in cancer progression, its specific roles and underlying mechanisms in gastric cancer (GC) remain poorly understood. We analysed SNORD3A expression using TCGA data and evaluated patient survival via Kaplan—Meier curves. Additionally, we conducted GO-KEGG enrichment analysis to identify relevant biological processes and signaling pathways, while ssGSEA was used to assess the correlation between SNORD3A and cancer immune infiltrates. Furthermore, we explored the relationship between SNORD3A and immunotherapy response through TIDE. We verified SNORD3A expression using real-time qPCR and assessed cell proliferation, migration, and invasion via CCK8 and Transwell migration and invasion assays.

Results: Our results revealed that SNORD3A was significantly upregulated in GC, with high expression correlating with poor survival. SNORD3A and related genes were primarily enriched in the insulin/insulin-related growth factor signaling pathway. We also observed negative associations between SNORD3A expression and several immune cells, including activated dendritic cells, CD56bright natural killer cells, central memory CD8 T cells, effector memory CD8 T cells, effector memory CD4 T cells, eosinophils, immature dendritic cells, macrophages, mast cells, MDSCs, memory B cells, monocytes, neutrophil cells, plasmacytoid dendritic cells, regulatory T cells, and T follicular helper cells. High SNORD3A expression also correlated with a poorer response to immunotherapy. Finally, inhibition of SNORD3A suppressed cell proliferation, migration, and invasion.

☆ Audio abstract available in Supplementary material.

* Corresponding authors.
E-mail addresses: qiwang1991331@foxmail.com (Q. Wang), 592363294@qq.com (J. Cao).

https://doi.org/10.1016/j.ejbt.2023.08.004

Conclusions: Our findings suggest that SNORD3A plays a catalytic role in the proliferation, migration and invasiveness of GC and may have potential as a diagnostic biomarker and therapeutic target for GC.
How to cite: Wang Q, Li Y, Niu X, et al. SNORD3A acts as a potential prognostic and therapeutic biomarker in gastric cancer. Electron J Biotechnol 2023; 67. https://doi.org/10.1016/j.ejbt.2023.08.004.

1. Introduction

As one of the most frequent gastrointestinal cancers, gastric cancer (GC) ranks fifth in cancer incidence and third in cancer mortality worldwide and causes serious social and medical burdens [1,2]. According to recent studies, the main risk factors associated with GC include Helicobacter pylori infection, Epstein-Barr virus infection, geographical location, smoking, and abnormal diet [3,4]. In the early stage of GC, gastrectomy is the prioritized strategy for the radical cure of patients [3,5]. Regardless of great enhancement in the survival rate of early GC patients, most GC patients show an advanced cancer stage without obvious symptoms at the time of diagnosis, which is usually associated with poor prognosis [6]. Understandably, early diagnosis and intervention may serve as the key to saving the lives of GC patients [6]. Currently, some tissue- and serum-based biomarkers are used for early-stage tumor screening and to predict disease progression or recurrence. Biomarkers widely used in clinical practice include CEA, AFP, CA724, and pepsinogen, but increasing evidence suggests that they have varying treatment effects and prognosis assessments. Therefore, it is essential to seek novel prognostic biomarkers that facilitate optimum treatment guidance and outcome prediction for GC patients.

SNORD3A belongs to a family of snoRNAs and is thought to play a role in the processing of ribosomal RNA precursors [7]. *SNORD3A* not only plays an important role in normal physiological functions but is also recognized as a novel oncogenic mRNA in many types of cancer [8,9,10]. Roychowdhury and coworkers found that *SNORD3A* was significantly downregulated in cervical carcinoma [8]. Godel et al. showed that SNORD3A reduced Dox cytotoxicity when overexpressed in Dox-sensitive cells [10]. Luo and colleagues verified that *SNORD3A* was significantly downregulated in breast cancer cells and tissues. Subsequent results indicated that Meis1-regulated *SNORD3A* specifically sensitized breast cancer cells to 5-FU by enhancing UMPS expression [9]. Irrespective of the important functions of *SNORD3A* in cancer development and progression, the potential roles and possible mechanisms of *SNORD3A* in GC are largely unclear.

In the current study, we identified that *SNORD3A* was significantly highly expressed in GC and that high expression of *SNORD3A* was associated with poor survival. We further explored the association of *SNORD3A* expression with distinct receptors and molecular pathways in GC. In addition, we also investigated the association between *SNORD3A* expression and the tumor immune microenvironment. Finally, we explored the role of *SNORD3A* silencing in the proliferation, migration, and invasion of GC cells.

2. Materials and methods

2.1. Data source

We downloaded the third-level RNA expression data and gene mutation data of gastric cancer as well as relevant clinical information, including patient sex, age, clinical stage, TNM stage, pathological type, tumor location, survival status, and total survival time from The Cancer Genome Atlas (TCGA, https://portal.gdc.cancer.gov/). After deleting incomplete clinical information cases, there were 368 gastric cancer samples and 32 normal samples.

2.2. Data processing

We obtained the RNA expression matrix after processing the downloaded RNA-seq data using R4.1.1 software. Subsequently, we used HTseq-TPM or counts to normalize the data according to the algorithm needs. Furthermore, we deleted the gene with 0 expression in all samples and retained the data with the largest mean value in all samples for the duplicate gene. Meanwhile, we extracted clinical information through R4.1.1 software to obtain clinical information, including sample number, age, sex, tumor stage and grade, tumor location, molecular subtype, total survival time, and survival status.

2.3. Relationship between SNORD3A expression and clinical information

First, we compared the expression of *SNORD3A* between normal and gastric cancer tissues. We utilized the 'survival' R package to calculate the optimal cut-off value for the SNORD3A expression level based on survival time, survival status, and the level of SNORD3A expression. Patients with SNORD3A expression levels below this cut-off value were categorized as the low-expression group, while those above it were classified as the high-expression group. Second, according to the expression of *SNORD3A* in gastric cancer samples, the "survival" R package was used to calculate the optimal cut-off value of *SNORD3A* expression, and then, the gastric cancer samples were divided into high and low expression *SNORD3A* groups. The "survival" package and "survival" package were used for survival analysis, and ggsurvivplot was used for survival analysis visualization. In addition, the differences in *SNORD3A* expression in different tumor locations were compared in different T stages, N stages, M stages and TNM stages, and the "ggplot2" package was used for boxplot visualization. Finally, the coxH command in the "survival" package was used to conduct multifactor Cox regression analysis with age, sex, TNM stage of gastric cancer, tumor grade, molecular subtypes of gastric cancer, and high and low expression groups of *SNORD3A*. The "forest-model" package was used to visualize the forest map.

2.4. Analysis of gene differences between high and low SNORD3A expression groups in gastric cancer

The "Dseq2" package of R 4.1.1 software was used to analyze the difference between the high and low expression groups of SNORD3A in all GC samples. The filter standard was |logFC|>1.5, and the corrected p value was < 0.05. The differential genes of the high and low expression groups of *SNORD3A* were obtained. The R 4.1.1 software "ggplot2" package was used to visualize the volcanic map of differential genes.

2.5. Functional enrichment analysis of differentially expressed genes

The R software "clusterProfiler" package was used to conduct gene ontology (GO) enrichment analysis and signal pathway

(Reactome) enrichment analysis for risk differential genes. Subsequently, we extracted the upregulated genes in the high *SNORD3A* expression group according to the logFC value, converted the gene ID into a human Entrez ID, and conducted GO enrichment analysis on the differentially expressed genes through the enrichGO command in the "cluster profiler" package. Moreover, we used the enrichPathway command to conduct enrichment analysis of the signal pathway (Reactome) and used the "ggplot2" package to visualize the enrichment results and draw a bubble diagram. We first conducted a correlation analysis between the insulin-like growth factor binding protein pathway genes and the expression levels of SNORD3A mRNA. We selected genes with a p value less than 0.05 and then performed univariate Cox regression analysis. Finally, we identified four genes that showed significant associations with survival. To further analyze the insulin-like growth factor-binding protein-related pathway enriched by the pathway, we carried out Spearman correlation analysis between the pathway-related gene and the expression of *SNORD3A* and then used "ggplot2" to visually draw the scatter diagram and fit the correlation straight line.

2.6. Evaluation of tumor microenvironment differences between high and low SNORD3A expression groups in gastric cancer

ssGSEA is a method commonly used in immune cell infiltration analysis that estimates the relative enrichment of a gene set in that sample by comparing the gene expression data of each sample to a specific gene set (immune cell gene set). In immune cell infiltration analysis, ssGSEA can be used to estimate the relative abundance of different immune cell types in each sample. Based on the gastric cancer RNA sequencing data, we used the gsva command in the "GSVA" package to conduct single-sample gene set enrichment analysis (ssGSEA) and obtained 28 immune cell enrichment scores for each gastric cancer sample. Immune cells refer to the cells involved in the immune response or related cells, including lymphocytes, dendritic cells, macrophages, granulocytes, and mast cells. Additionally, the matrix score, immune score, ESTIMATE score and tumor purity of each sample were calculated using the same method (estimation of normal and immune cells in malignant tumor tissues using expression data, ESTIMATE). We used the "ComplexHeatmap" package and "ggplot2" package to visualize and draw the differential heatmap of immune cell infiltration and the differential boxplot of immune cell infiltration in the high and low *SNORD3A* groups. Finally, Spearman correlation analysis was used to explore the correlation between the expression of immune checkpoint-related genes and *SNORD3A*, followed by visualization using the "ComplexHeatmap" package.

2.7. SNORD3A and immunotherapy

The immune treatment response of all samples was assessed using tumor immune dysfunction and exclusion (TIDE) (https://tide.dfci.harvard.edu/). The heatmap of relevant indicators of immunotherapy was visualized using the "ComplexHeatmap" package. We used the "ggplot2" package to visualize the proportion of effective immunotherapy in the high and low expression SNORD3A groups.

2.8. Gene mutation analysis

The "IOBR" package was used to evaluate the gene mutations of NK cells, CD8+ T cells and immunosuppressive markers in all samples. The waterfall chart shows the top 10 genes with a mutation frequency. The relationship between gene mutations and *SNORD3A* expression was further analyzed, and "ggplot2" was used to visualize and draw a box diagram of gene mutations and *SNORD3A* expression.

2.9. Drug sensitivity prediction

The CellMiner database was used to evaluate the semi-inhibitory concentration (IC50) of each sample to predict the drug sensitivity of each sample. Spearman correlation analysis was performed using the previously analyzed genes related to the insulin-like growth factor binding protein pathway and the genes significantly related to the expression of *SNORD3A* and the drug IC50. "ggplot2" was used to visually draw the scatter diagram and fit the correlation line.

2.10. Cell culture and plasmid transfection

The AGS and HCG27 cell lines were used in this study because they are human gastric cancer cell lines. All GC cells were cultured in 1640 medium containing 10% fetal bovine serum. GC cells were transfected with si-NC (negative control) and si-*SNORD3A*. si-*SNORD3A* (small-interfering RNAs against SNORD3A) was used to knock down *SNORD3A*. The siRNA sequence is provided in Table S1. All plasmids were purchased from GenePharma (Shanghai, China).

2.11. Real-time quantitative PCR

Total RNA was extracted using TRIzol (Invitrogen, USA) according to previous methods. The real-time quantitative PCR (RT-qPCR) procedure was then completed. The experiments were repeated 3 times. The primers were as follows: SNORD3A (forward primer: 5′-CGGTGACGGCTCTTGGGTTT-3′, reverse primer: 5′-CGGGAAACG GCGACAAAA-3′) and GAPDH (forward primer: 5′-AATGGG CAGCCGTTAGGAAA-3′, reverse primer: 5′-GCCCAATACGACCAAAT CAGAG-3′).

2.12. Cell proliferation assay

The CCK-8 kit was used for rapid and sensitive detection of cell proliferation and cytotoxicity. The working principle is as follows: in the presence of electron compound reagents, WST-8 (chemical name: 2-(2-methoxy-4-nitrophenyl)-3-(4-nitrophenyl)-5-(2,4-disulfonobenzene)-2h-tetrasomonodium salt) can be reduced by mitochondrial dehydrogenase to produce a highly water-soluble orange-yellow product (formazan), the depth of which is proportional to cell proliferation and inversely proportional to cytotoxicity. OD values measured at 450 nm wavelength by an enzymoleter can indirectly reflect the number of living cells. After a 24-h culture period with different siRNAs, the absorbance at 450 nm was measured after adding 10 μL of CCK-8 reagent (Dojindo Company, Beijing, China). After being scraped to create a 1-mm gap, the cells treated with different siRNAs were grown for 48 h, and images were obtained at 0 and 48 h.

The EdU assay was performed as follows: Logarithmically growing cells were seeded into a 96-well plate and treated with a 50 μM 5-ethynyl-2′-deoxyuridine (EdU) stock solution at 37°C for 2 h. The cells were then fixed with 4% paraformaldehyde (PFA), and the nuclei were stained with DAPI (D9542, Sigma-Aldrich). The resulting fluorescence was captured using an Olympus microscope.

The colony formation assay was conducted to determine the proliferation ability of cells. The rate of cell colony formation represents the number of adherent cells surviving and forming clones after inoculation, which can reflect two important traits of cell population dependence and proliferation ability. By observing the formation of single-cell colonies, we can calculate the colony formation rate and understand its proliferation ability. The cells were

seeded in a 6-well plate at a density of 500–1000 cells per well and grown for 2–3 weeks until macroscopic colonies were observed. The colonies were then washed with PBS, fixed with 4% paraformaldehyde for 20 min, and stained with 1% crystal violet for 10 min. The colony formation rate was calculated by dividing the number of colonies by the number of seeded cells.

2.13. Cell migration and invasion assays

Transwell migration and invasion assays refer to the transwell chamber placed in the culture plate, the upper chamber is called the small chamber, the lower chamber is called the culture plate, the upper and lower culture medium are separated by polycarbonate vinegar film, and the cells under study are planted in the upper chamber. Due to the permeability of the polycarbonate membrane, the components of the lower culture medium can affect the cells in the upper chamber. With the application of different pore sizes and different treatments of polycarbonate vinegar film, it can be studied in many aspects, such as coculture, cell chemotactic cell migration, and cell invasion. For the transwell migration assay, logarithmically growing cells suspended in serum-free medium were placed in the upper chamber of each insert (Corning, Cambridge, USA) that contained a noncoated membrane or hydrated Matrigel chambers (50 μL). The lower chambers were supplemented with 600 μL of 10% fetal bovine serum. After a 24-h incubation period at 37°C, the cells on the upper surface were then scraped away, and the cells on the lower surface were fixed, stained with 0.1% crystal violet for 30 min, and visualized.

A wound healing assay was conducted to estimate cell migration. Cells were seeded onto 6-well plates, and a scratch was created using a 200 μL tip. Then, we observed the expansion of wound closure, and the cell coverage crossing the line was measured to evaluate the migration rate. ImageJ software was used to measure the scratch blank area to assess cell coverage.

2.14. Cell apoptosis analysis

Apoptotic cells were analyzed by flow cytometry (UTHSCSA, Flow Cytometry Core). The cells were collected and resuspended in binding buffer (Procell Life Science & Technology Co.) and stained with the Annexin V-APC/PI Apoptosis Detection Kit (KeyGEN, China). The percentage of cells in the "Q2 + Q3" gate was considered the apoptotic rate.

2.15. Statistical analysis

The "Dseq2" package of R 4.1.1 software was used to analyze the difference between the high and low expression groups of SNORD3A in all GC samples. The filter standard was |logFC|>1.5, and the corrected p value was <0.05. We selected genes with a p value less than 0.05 and then performed univariate Cox regression analysis. Student's t test was used in statistical analyses and performed by SPSS 26.0 software. All experiments were repeated three times. A value of 0.05 or less was considered significant.

3. Results

3.1. SNORD3A expression was higher in gastric cancer

First, we analyzed the expression level of *SNORD3A* in pancancer. By analyzing the TCGA data, we found significant differences in the high expression of SNORD3A in various cancers, including adrenocortical carcinoma (ACC), invasive breast carcinoma (BRCA), kidney renal papillary cell carcinoma (KIRP), brain lower grade glioma (LGG), liver hepatocellular carcinoma (LIHC), pancreatic adenocarcinoma (PAAD), colon adenocarcinoma (COAD), lymphoid neoplasm diffuse large B-cell lymphoma (DLBC), esophageal carcinoma (ESCA), glioblastoma multiforme (GBM), head and neck squamous cell carcinoma (HNSC), ovarian cancer (OV), prostate adenocarcinoma (PRAD), thyroid carcinoma (THCA), uterine carcinosarcoma (UCS), lung squamous cell carcinoma (LUSC), rectum adenocarcinoma (READ), stomach adenocarcinoma (STAD), thymoma (THYM), skin cutaneous melanoma (SKCM) and uterine corpus endometrial carcinoma (UCEC) (Fig. 1A). Specifically, we found that SNORD3A was more highly expressed in tumor tissues than in normal tissues of GC and that high expression of SNORD3A was associated with poor overall survival (Fig. 1B). Collectively, our data indicated that SNORD3A is more highly expressed in GC.

3.2. Overexpression of SNORD3A was related to poor prognosis in gastric cancer

Then, we analyzed the correlation between the expression of *SNORD3A* and clinical pathologic characteristics in GC. The expression of *SNORD3A* was highest in T3, N3, M0, and stage 3. Other characteristics showed no significant differences (Fig. 1C-G). In further multivariate analysis, high *SNORD3A* expression was proven to be independently prognostic for worse OS in patients aged > 65, male patients, stage 4 patients, and patients with high *SNORD3A* expression (Fig. 1H).

3.3. Enrichment analysis of SNORD3A expression-related genes in gastric cancer

To explore the potential functional roles of *SNORD3A*, functional enrichment analysis was performed based on GO pathway analysis. We divided GC patients into *SNORD3A*-high expression and SNORD3A-low expression groups in TCGA data. Differential expression analysis identified that a total of 357 genes were significantly higher and 512 genes were downregulated (Fig. 2A). Pathway analysis indicated that these genes were mainly enriched in the insulin/insulin-related growth factor (IGF) signaling pathway, olfactory signaling pathway, and GPCR ligand binding (Fig. 2B). GO analysis showed that these genes were mainly enriched in sensory perception of smell, detection of chemical stimulus involved in sensory perception, organic anion transport, olfactory receptor activity, signaling receptor activator activity and receptor ligand activity (Fig. 2C-D). Considering that the IGF signaling pathway participates in the development and progression of GC, we selected it for subsequent analysis [11,12]. The correlation analysis showed that *SNORD3A* was negatively correlated with the expression of CALU and FAM20A but positively correlated with PLG and SERPINC1 (Fig. 2E-H). We also conducted survival analysis for the four IGF signaling pathway-associated genes based on TCGA data. Survival analysis indicated that high expression of CALU, FAM20A, PLG, and SERPINC1 was associated with poorer overall survival (Fig. 2I-L).

3.4. The correlation between SNORD3A and immune infiltration in gastric cancer

Previous studies indicated that the tumor immune microenvironment plays critical roles in the onset and progression of GC [13,14,15], so we tried to explore the correlation between *SNORD3A* and immune cell infiltration and immune checkpoints in GC. We characterized the infiltration patterns of 28 immune cell types in the tumor microenvironment of GC using ssGSEA. (Fig. 3A). We found that the expression of SNORD3A was negatively associated with activated dendritic cells, CD56 bright natural killer cells, central memory CD8+ T cells, effector memory CD8+ T cells,

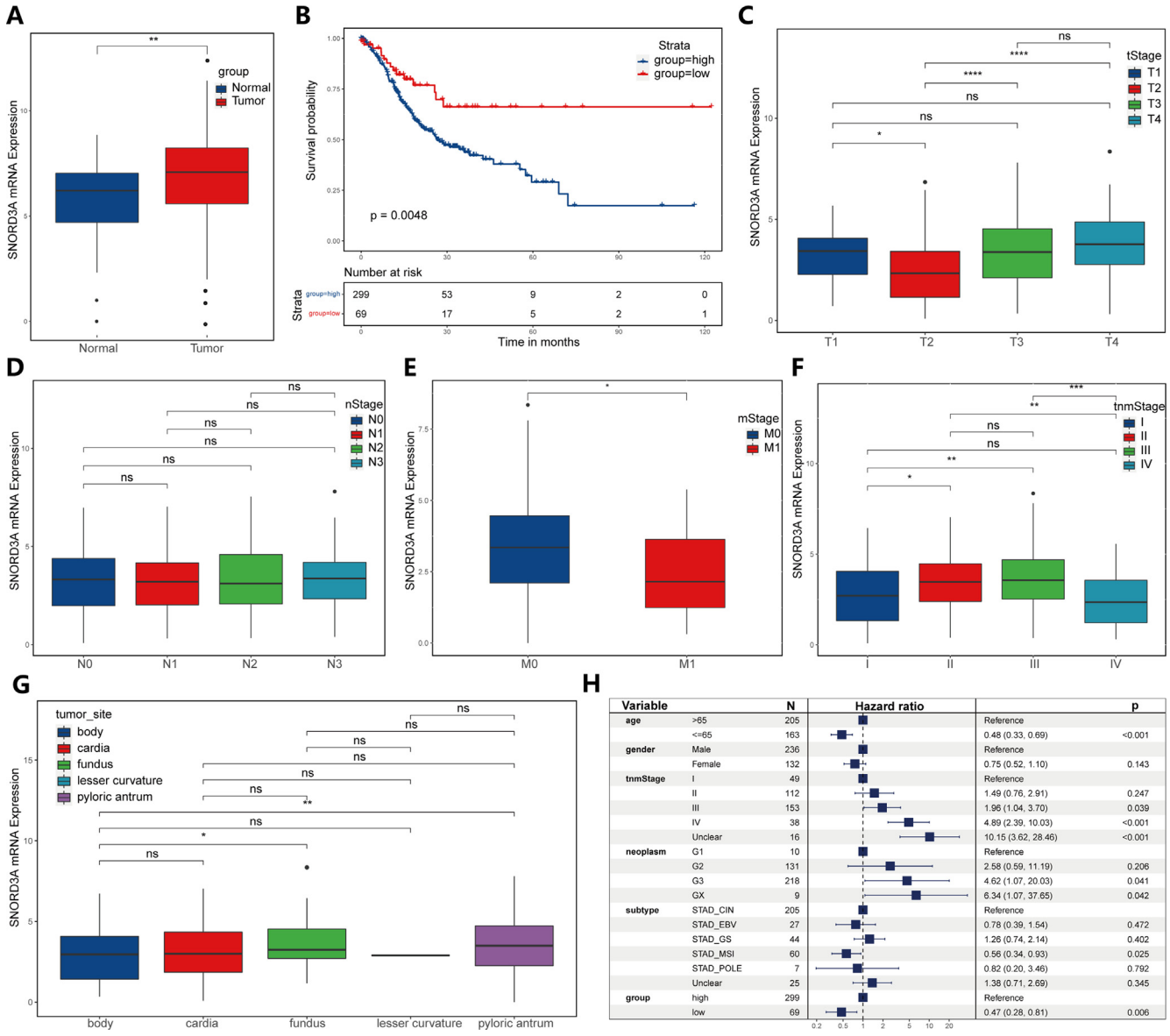

Fig. 1. The SNORD3A mRNA expression level was significantly correlated with advanced clinicopathological parameters and poor survival outcomes in GC patients from the TCGA cohort. (A). Pancancer analysis of SNORD3A expression levels in cancerous and normal tissues. (B). Survival analysis by the Kaplan–Meier method indicated that SNORD3A was significantly correlated with shorter OS (p = 0.0048). (C-G). The mRNA expression level of SNORD3A was significantly correlated with AJCC stage and tumor site. (H). Forest plot of multivariate regression analyses showing the association between SNORD3A mRNA expression level and patient survival.

effector memory CD4+ T cells, eosinophils, immature dendritic cells, macrophages, mast cells, MDSCs, memory B cells, monocytes, neutrophil cells, plasmacytoid dendritic cells, regulatory T cells, and T follicular helper cells (Fig. 3B). Additionally, we determined the immunization score in the SNORD3A-high expression and SNORD3A-low expression groups using ESTIMATE. We found that patients with low SNORD3A expression had higher stromal scores, immune scores, and ESTIMATE scores and lower tumor purity (Fig. 3C). Furthermore, immune checkpoint analysis showed that SNORD3A was negatively associated with the expression of HAVCR2 and PDCD1LG2 (Fig. 3D, Fig. S1).

3.5. The correlation between SNORD3A and immunotherapy response in gastric cancer

We also analyzed the relationship between SNORD3A and immunotherapy response in GC. Using the TIDE algorithm, we identified that patients in the high-expression SNORD3A group showed a worse immunotherapy response (Fig. 4A-B). Considering the critical roles of NK cells, $CD8^{+}$ cells and immune checkpoints in the immunotherapy response, we also performed gene mutation analysis of these signatures (Fig. 4C-D and Fig. S2A-B). Some gene mutations were shown in the NK cell cytotoxicity signature, including *TTN, TP53, PIK3CA, ARID1A, PLXNA4, CDH1, SPEG, MAGEC1, TRPA1,* and *LAMA3*. Some gene mutations were found in $CD8^{+}$ T cells, including *PIK3CA, PLEC, DMD, TCHH, ARID1A, ANK3, PLXNA4, WDFY3, LRP1* and *SPEG* (Fig. S1A). Some gene mutations were shown in immune checkpoints, including *PIK3CA, AHNAK2, ARID1A, ANK3, RNF213, TCHH, PLXNA4 ABCC9* LRP1 and *SPEG* (Fig. S2B). Further detection of the expression level of *SNORD3A* in wild-type and mutant genomes showed that the expression level of *SNORD3A* was significantly increased in the mutant genomes of *ABCB1, CNTN1, PLEC* and *USP34* (Fig. 4E-H).

3.6. Prediction of potential anticancer drugs

To further investigate the clinical use of *CALU* and *SERPINC1*, the CellMiner database was employed to explore the relationship

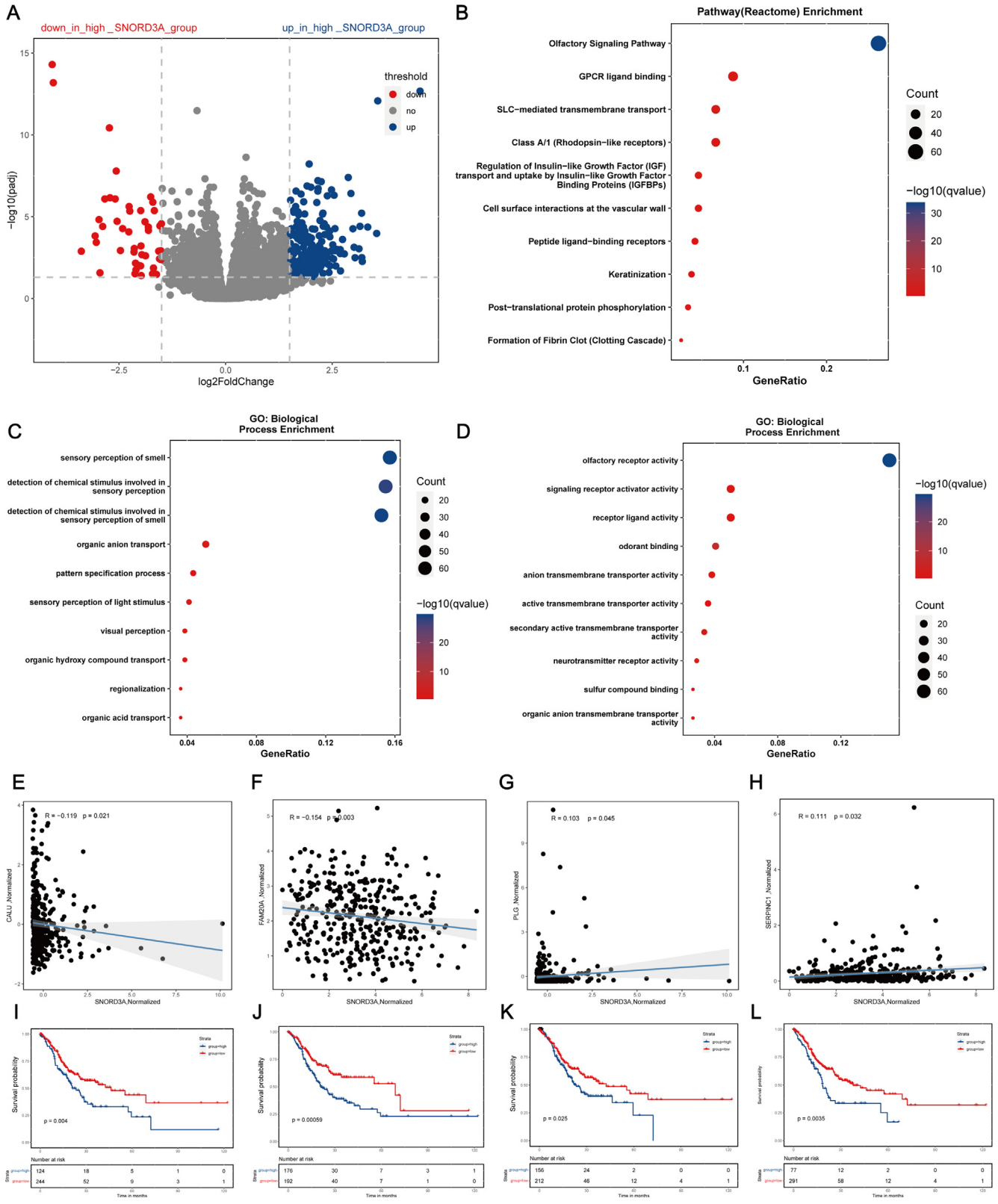

Fig. 2. Identification of DEGs based on SNORD3A expression level and related functional annotations. (A). Analysis of DEGs based on SNORD3A mRNA expression level (p adj < 0.05, |log2(fold change)| >2. Reactome pathway enrichment analysis. (C-D). GO enrichment analysis. (E-H). Analysis of the correlation between gene expression of the insulin/insulin-related growth factor signaling pathway and SNORD3A expression. (I-L) Survival analysis of genes related to SNORD3A in the insulin/insulin-related growth factor signaling pathway.

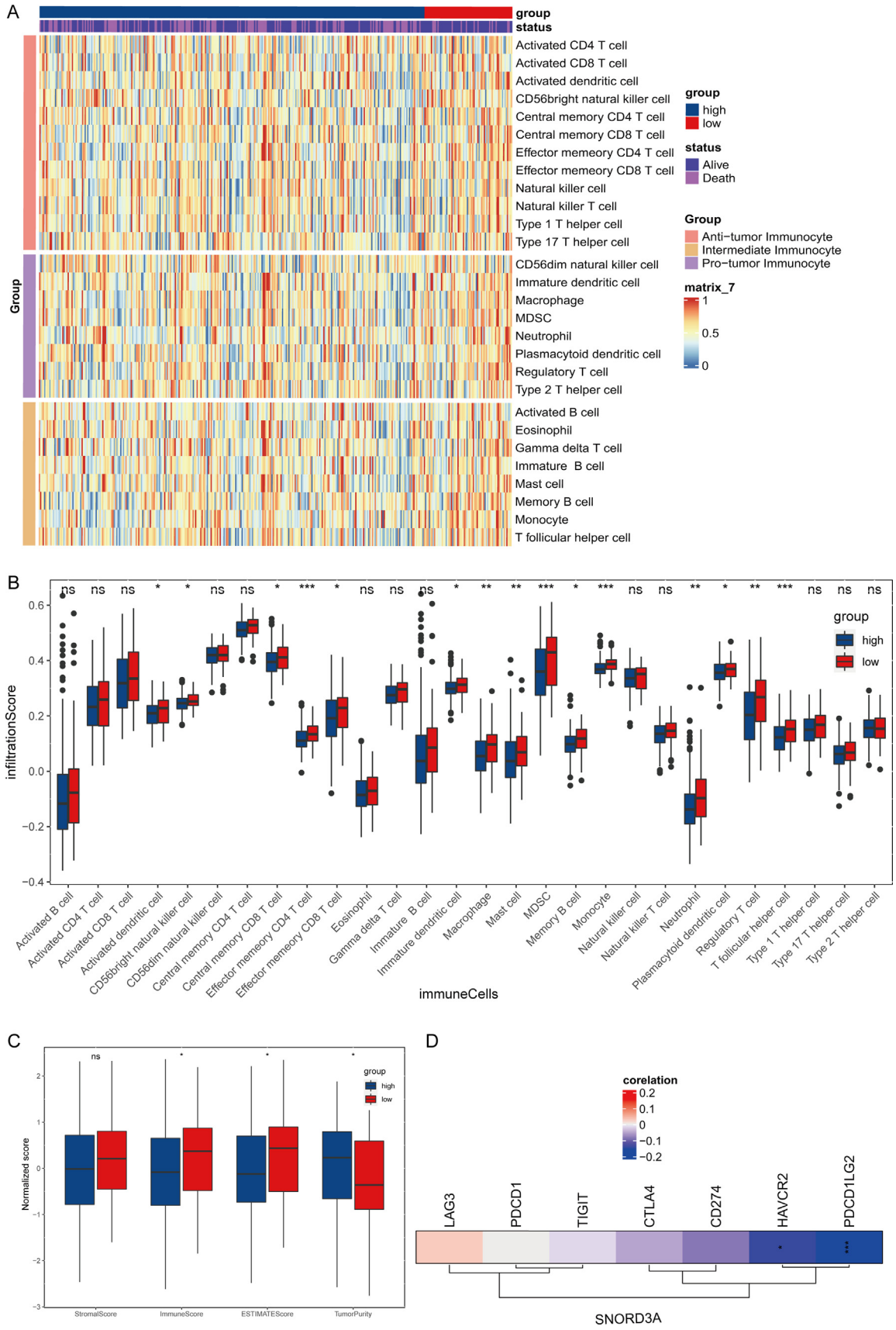

Fig. 3. The relationship between SNORD3A expression level and immune infiltration pattern in the tumor microenvironment. (A-B). Differences in immune cell infiltration between the high- and low-SNORD3A groups. (C) Stroma score, immune score, ESTIMATE score, and tumor purity between the high- and low-SNORD3A groups based on the ESTIMATE algorithm. (D) Correlation between SNORD3A expression level and immune checkpoint-related genes.

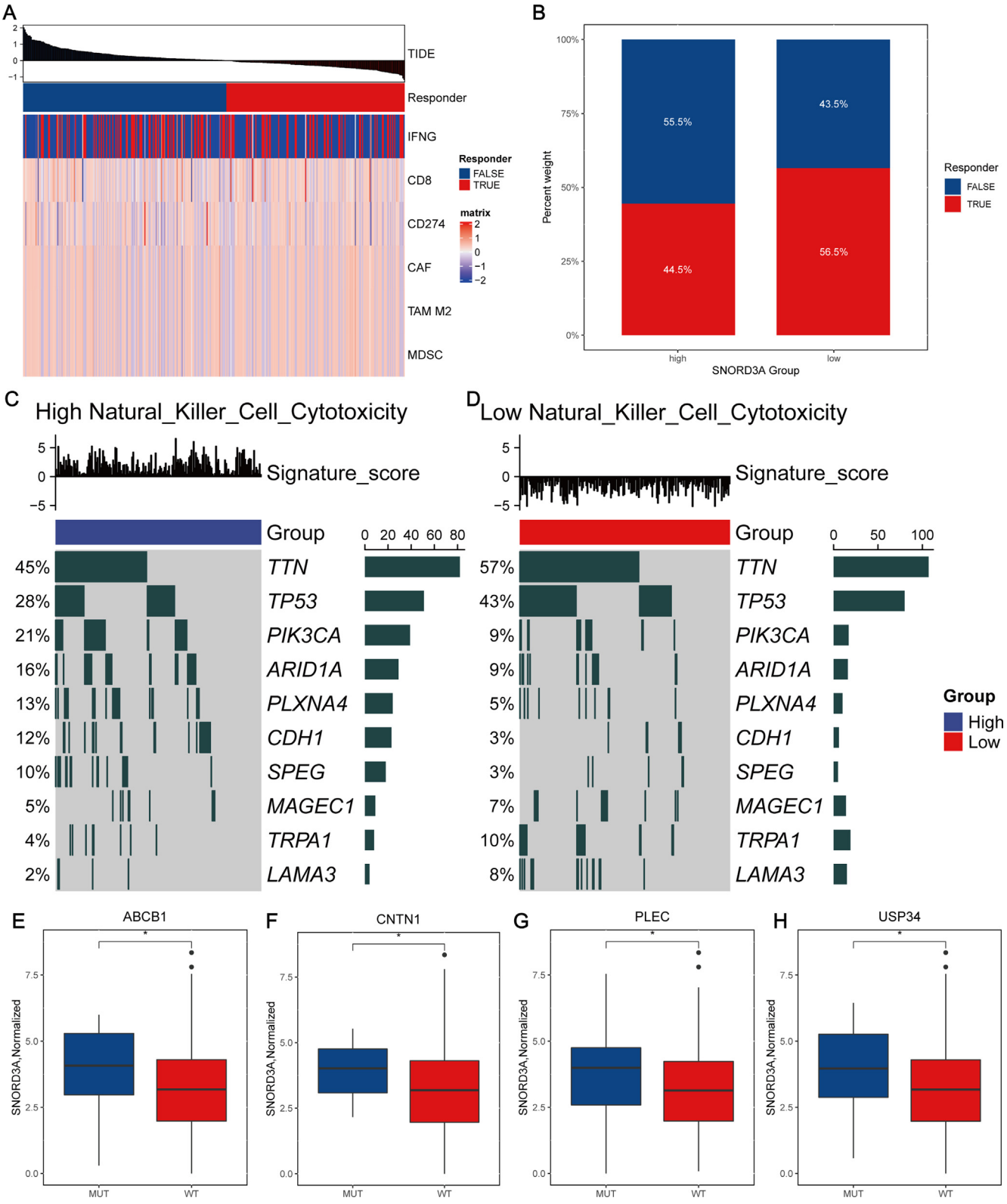

Fig. 4. The relationship between SNORD3A expression level and immunotherapy for GC. (A). Correlation between TIDE score in GC and immunotherapy. (B). Differences in the immune therapy response rate between the high- and low-SNORD3A groups. (C-D). High-frequency mutated genes in the high- and low-NK cell-related signature score groups. (E-H). The relationship between gene mutations and SNORD3A expression level.

between these genes and drug sensitivity. *CALU* was inversely associated with the following drug sensitivities: Aloin (correlation = −0.45, P < 0.001), Ergosterol (correlation = −0.35, P < 0.001), Ribavirin (correlation = −0.51, P < 0.001) and Dexamethasone_Decadron (correlation = −0.47, P < 0.001) (Fig. 5A-C, E). *CALU* was positively associated with sensitivity to nitazoxanide

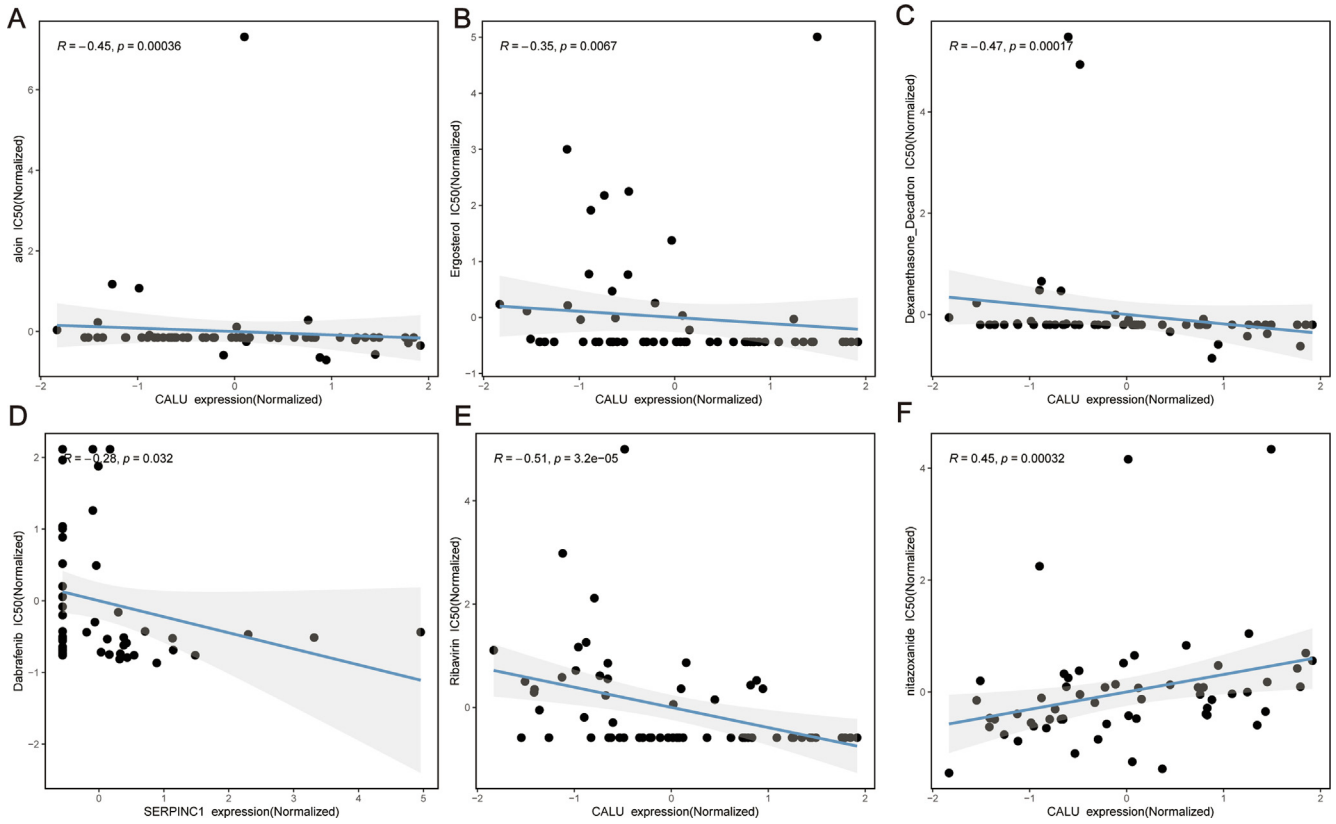

Fig. 5. Drug sensitivity analysis. (A-F). Correlation between SNORD3A expression level and drug IC50 values.

(correlation = 0.45, P < 0.001) (Fig. 5F). Moreover, *SERPINC1* was positively associated with the following drug sensitivities: dabrafenib (correlation = −0.28, P = 0.032) (Fig. 5D).

3.7. SNORD3A was higher in gastric cancer, promoted cell Proliferation, migration and invasion and inhibited apoptosis in GC cells

To better explore the functional roles of *SNORD3A* in GC, we constructed *SNORD3A* knockdown GC cell lines using siRNA. The qRT-PCR results verified that the expression of *SNORD3A* was significantly knocked down using siRNA (Fig. 6A). The results of CCK-8 (Fig. 6B), EdU (Fig. 6E), and colony formation (Fig. 6F) assays showed that inhibition of *SNORD3A* significantly suppressed GC cell proliferation. The results of the Transwell assay (Fig. 6C-D) and wound healing assays (Fig. 6G-I) showed that cell migration and invasion were also suppressed in GC cell lines treated with siSNORD3A. Moreover, the results of the cell apoptosis assay showed that inhibition of *SNORD3A* significantly reduced GC cell apoptosis (Fig. 6H). Taken together, our findings indicated that *SNORD3A* positively regulates cell proliferation, migration, invasion and apoptosis in GC.

4. Discussion

Gastric cancer (GC) is one of the most common gastrointestinal cancers worldwide, particularly in Asia. Despite significant progress in the diagnosis and treatment of GC, including advanced GC, prognosis remains poor due to unclear mechanisms underlying its development and progression. In this study, we found that *SNORD3A* plays a catalytic role in the proliferation, migration and invasiveness of GC and may have potential as a diagnostic biomarker and therapeutic target for GC.

SNORD3A plays an important role in the processing of ribosomal RNA precursors. Previous studies have shown that *SNORD3A* is differentially expressed in various malignant cancers and is associated with malignant pathological processes, including the proliferation, invasion, migration, and chemoresistance of tumor cells [8,9,10].

The results of our study suggest that *SNORD3A* may serve as a potential diagnostic and therapeutic target in cancer diagnosis and treatment. We found that *SNORD3A* was significantly overexpressed in GC, and its high expression was associated with pathological features and poor overall survival. Additionally, we observed that inhibition of *SNORD3A* suppressed GC cell proliferation, invasion, and migration. Our findings support the use of *SNORD3A* as an independent prognostic predictor and biomarker in patients with GC.

We further performed functional enrichment analysis for *SNORD3A*-associated genes in our study. The enrichment analysis of GO and KEGG revealed that the high expression of *SNORD3A* is related to the insulin/insulin-related growth factor (IGF) signaling pathway, olfactory signaling pathway, and GPCR ligand binding. An increasing number of studies have shown that the IGF signaling pathway plays a critical role in the occurrence and development of many malignant tumors, including breast cancer, non-small cell lung cancer, and hepatoblastoma [16,17]. For instance, Lee et al. found that the insulin and IGF signaling pathways promoted breast cancer stem cells through IRS2/PI3K-mediated regulation of MYC [18]. Zhen and coworkers revealed that circHMGCS1 facilitated hepatoblastoma cell proliferation by regulating the IGF signaling pathway and glutaminolysis [19]. Du and colleagues demonstrated that inhibition of the IGF signaling pathway reversed cisplatin resistance in ovarian cancer cells [20]. Additionally, several studies have shown that the IGF signaling pathway participates in the pathogenesis of GC. Saisana and colleagues revealed that insulin

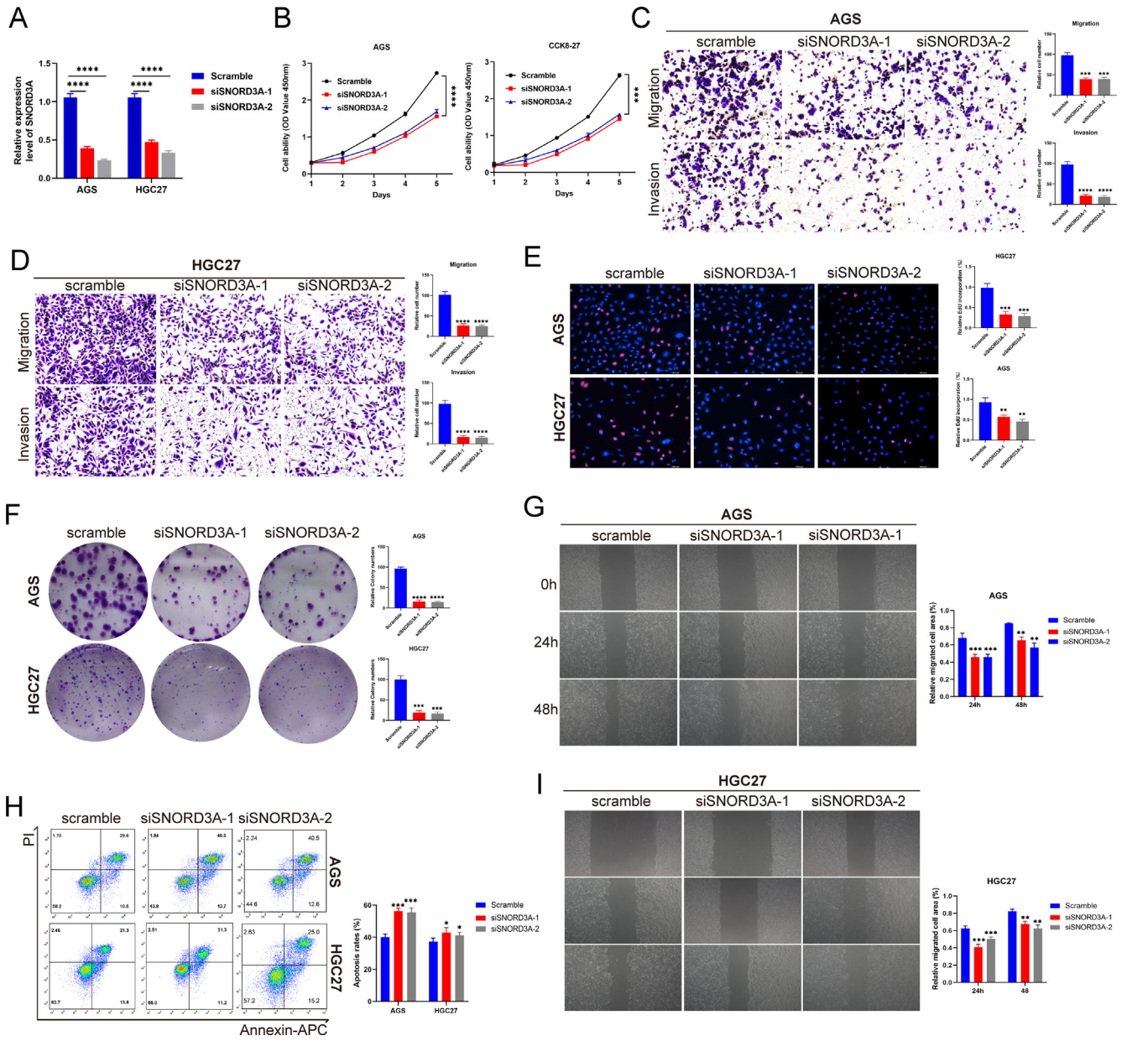

Fig. 6. SNORD3A promotes the proliferation, invasion, and migration of gastric cancer cells. (A). Validation of the efficiency of SNORD3A knockdown in GC cells by qRT-PCR. (B, E, F). Knocking down SNORD3A suppressed the proliferative ability of GC cells. (C, D) Downregulating SNORD3A inhibits GC cell migration and invasion. (G, I) Downregulating SNORD3A inhibits GC cell wound healing ability. (H) Silencing SNORD3A expression inhibited the anti-apoptotic capacity of GC cells.

and the insulin receptor collaborate to promote the progression of GC [21]. Several carcinomas, including GC, have been verified to be involved in Epstein-Barr virus (EBV) infection. Jeong et al. showed that AGS-EBV cells regulated their proliferation and invasion through the IGF signaling pathway [22]. The olfactory signaling pathway has been implicated in various physiological and pathological processes, including neurogenesis, inflammation, and tumorigenesis. However, its role in GC requires further investigation. Additionally, G protein-coupled receptor (GPCR) ligand binding has been associated with various biological processes, such as cellular communication, sensory perception, and immune response. Our study sheds light on the potential involvement of *SNORD3A* in regulating these signaling pathways and provides insights into the molecular mechanisms underlying GC pathogenesis. Future research is needed to further explore the specific roles of *SNORD3A* in these pathways and their clinical implications for GC diagnosis and treatment.

Recent years have seen significant advancements in tumor and molecular biology, leading to the discovery that the tumor microenvironment (TME) plays a critical protumorigenic role [23]. The TME consists of various cell types, including immune cells, fibroblasts, endothelial cells, and adipocytes, as well as extracellular matrix components and signaling molecules. The TME exerts its effects through cytokines and growth factors that support cancer cell proliferation, survival, motility, and invasion. Studies have shown that the TME is involved in the initiation, progression, and metastasis of many cancers, including gastric cancer. In GC, the TME has been shown to contribute to drug resistance, immune evasion, and angiogenesis. Moreover, recent research has suggested that targeting the TME may provide novel

therapeutic strategies for GC treatment. Our study found that *SNORD3A* can affect the immune microenvironment of GC cells. Using the CIBERSORT algorithm, we identified that SNORD3A was negatively associated with activated dendritic cells, CD56bright natural killer cells, central memory CD8 T cells, effector memory CD8 T cells, effector memory CD4 T cells, eosinophils, immature dendritic cells, macrophages, mast cells, MDSCs, memory B cells, monocytes, neutrophil cells, plasmacytoid dendritic cells, regulatory T cells, and T follicular helper cells. Therefore, we could infer that SNORD3A may influence the transition of TME status and that the role of SNORD3A in the TME should be considered in GC treatment. In recent years, immune checkpoint inhibitors and immunotherapy have gained increasing attention in the treatment of gastric cancer (GC). Immune checkpoint inhibitors work by blocking the inhibitory signals that prevent T cells from attacking cancer cells [24,25] Accordingly, we also explored the correlation between SNORD3A and immune checkpoints and immunotherapy response. Immune checkpoint analysis showed that *SNORD3A* was negatively associated with the expression of *HAVCR2* and *PDCD1LG2*, which suggested that *SNORD3A* may be a promising immune checkpoint indicator. Immunotherapy response analysis showed that patients in the high *SNORD3A* expression group showed a worse immunotherapy response. Afterwards, we will further clarify the underlying molecular mechanisms of *SNORD3A* in the regulation of immune checkpoints and immunotherapy responses.

In this study, we investigated the potential association between *SNORD3A* and GC. Although our findings suggest a correlation between *SNORD3A* expression and GC progression, there are still some limitations that must be addressed in future studies. First, the data used in this study were obtained from public databases. Therefore, further validation studies using our own cohort data are necessary to confirm our results. A larger sample size would also ensure greater accuracy and reliability of our findings.

Second, while we performed several bioinformatic analyses, including expression analysis, functional enrichment analysis, and immune microenvironment analysis, we only conducted RNA interference experiments to examine the roles of *SNORD3A* in GC cell proliferation, invasion, and migration. Further studies are needed to investigate the functions of *SNORD3A* in GC *in vitro* and *in vivo*. This would provide a more comprehensive understanding of the role of *SNORD3A* in GC. Finally, although we explored the potential molecular mechanisms of *SNORD3A* in GC, future research should focus on elucidating the direct mechanisms. It is important to identify the specific pathways or molecules that *SNORD3A* regulates in GC progression. This will allow researchers to develop targeted therapies for GC patients. In future studies, it would be beneficial to conduct validation studies using our own cohort data to confirm the results obtained in this study. Additionally, functional studies investigating the effects of *SNORD3A* on GC cell proliferation, invasion, and migration in vitro and in vivo should be conducted. Finally, the specific pathways and molecules that *SNORD3A* regulates should be identified to develop targeted therapies for GC patients.

Despite the limitations of this study, our findings suggest a correlation between *SNORD3A* expression and GC progression. Further studies are necessary to validate our results, investigate the functions of *SNORD3A* in GC, and identify the specific pathways or molecules that *SNORD3A* regulates. This will provide a better understanding of the role of *SNORD3A* in GC and contribute to the development of targeted therapies for GC patients.

Authors' Contributions

- Study conception and design: Q Wang, Y Li.
- Data collection: X Niu, C Zhang.
- Analysis and interpretation of results: J Zhang, J Cao, L Wu.
- Draft manuscript preparation: Q Wang, Y Li.
- Revision of the results and approved the final version of the manuscript: Q Wang, J Cao, L Wu.

Financial support

None.

Conflicts of interest

The authors declare that they have no conflicts of interest.

Data availability

The data will be available upon reasonable request.

Supplementary material

https://doi.org/10.1016/j.ejbt.2023.08.004.

References

[1] Sung H, Ferlay J, Siegel RL, et al. Global cancer statistics 2020: GLOBOCAN estimates of incidence and mortality worldwide for 36 cancers in 185 countries. CA Cancer J Clin 2021;71(3):209–49. https://doi.org/10.3322/caac.21660. PMID:33538338.
[2] Ajani JA, D'Amico TA, Bentrem DJ, et al. Gastric cancer, Version 2.2022, NCCN clinical practice guidelines in oncology. J Natl Compr Canc Netw 2022;20(2):167–92. https://doi.org/10.6004/jnccn.2022.0008. PMID:35130500.
[3] Smyth EC, Nilsson M, Grabsch HI, et al. Gastric cancer. Lancet 2020;396(10251):635–48. https://doi.org/10.1016/s0140-6736(20)31288-5. PMID:32861308.
[4] Tsao SW, Tsang CM, Pang PS, et al. The biology of EBV infection in human epithelial cells. Semin Cancer Biol 2012;22(2):137–43. https://doi.org/10.1016/j.semcancer.2012.02.004. PMID:22497025.
[5] Li GZ, Doherty GM, Wang J. Surgical management of gastric cancer: A review. JAMA Surg 2022;157(5):446–54. https://doi.org/10.1001/jamasurg.2022.0182. PMID:35319717.
[6] Alsina M, Arrazubi V, Diez M, et al. Current developments in gastric cancer: from molecular profiling to treatment strategy. Nat Rev Gastroenterol Hepatol 2022;20:155-170. https://doi.org/10.1038/s41575-022-00703-w. PMID:36344677.
[7] Zhang X, Wang C, Xia S, et al. The emerging role of snoRNAs in human disease. Genes Diseases 2023;10(5):2064–81. https://doi.org/10.1016/j.gendis.2022.11.018. PMID: 37492704.
[8] Roychowdhury A, Samadder S, Das P, et al. Deregulation of H19 is associated with cervical carcinoma. Genomics 2020;112(1):961–70. https://doi.org/10.1016/j.ygeno.2019.06.012. PMID:31229557.
[9] Luo L, Zhang J, Tang H, et al. LncRNA SNORD3A specifically sensitizes breast cancer cells to 5-FU by sponging miR-185-5p to enhance UMPS expression. Cell Death Dis 2020;11(5):329. https://doi.org/10.1038/s41419-020-2557-2. PMID:32382150.
[10] Godel M, Morena D, Ananthanarayanan P, et al. Small nucleolar RNAs determine resistance to doxorubicin in human osteosarcoma. Int J Mol Sci 2020;21(12):4500. https://doi.org/10.3390/ijms21124500. PMID:32599901.
[11] Wang G, Lu M, Yao Y, et al. Esculetin exerts antitumor effect on human gastric cancer cells through IGF-1/PI3K/Akt signaling pathway. Eur J Pharmacol 2017;814:207–15. https://doi.org/10.1016/j.ejphar.2017.08.025. PMID:28847482.
[12] Guo C, Chu H, Gong Z, et al. HOXB13 promotes gastric cancer cell migration and invasion via IGF-1R upregulation and subsequent activation of PI3K/AKT/mTOR signaling pathway. Life Sci 2021;278:119522. https://doi.org/10.1016/j.lfs.2021.119522. PMID:33894267.
[13] Kim R, An M, Lee H, et al. Early tumor-immune microenvironmental remodeling and response to first-line fluoropyrimidine and platinum chemotherapy in advanced gastric cancer. Cancer Discov 2022;12(4):984–1001. https://doi.org/10.1158/2159-8290.Cd-21-0888. PMID:34933901.
[14] Shi T, Zhang Y, Wang Y, et al. DKK1 Promotes tumor immune evasion and impedes Anti-PD-1 treatment by inducing immunosuppressive macrophages

in gastric cancer. Cancer Immunol Res 2022;10(12):1506–24. https://doi.org/10.1158/2326-6066.Cir-22-0218. PMID:36206576.
[15] Gambardella V, Castillo J, Tarazona N, et al. The role of tumor-associated macrophages in gastric cancer development and their potential as a therapeutic target. Cancer Treat Rev 2020;86:102015. https://doi.org/10.1016/j.ctrv.2020.102015. PMID:32248000.
[16] Saisana M, Griffin SM, May FEB. Importance of the type I insulin-like growth factor receptor in HER2, FGFR2 and MET-unamplified gastric cancer with and without Ras pathway activation. Oncotarget 2016;7(34):54445–62. https://doi.org/10.18632/oncotarget.10642. PMID:WOS:000385435000029.
[17] Choi YJ. Insulin resistance: A hidden risk factor for gastric cancer? Gut Liver 2019;13(2):133–4. https://doi.org/10.5009/gnl19060. PMID:30893982.
[18] Lee JS, Lero MW, Mercado-Matos J, et al. The insulin and IGF signaling pathway sustains breast cancer stem cells by IRS2/PI3K-mediated regulation of MYC. Cell Rep 2022;41(10):111759. https://doi.org/10.1016/j.celrep.2022.111759. PMID:36476848.
[19] Zhen N, Gu S, Ma J, et al. CircHMGCS1 promotes hepatoblastoma cell proliferation by regulating the IGF signaling pathway and glutaminolysis. Theranostics 2019;9(3):900–19. https://doi.org/10.7150/thno.29515. PMID:30809316.
[20] Du J, Shi HR, Ren F, et al. Inhibition of the IGF signaling pathway reverses cisplatin resistance in ovarian cancer cells. BMC Cancer 2017;17(1):851. https://doi.org/10.1186/s12885-017-3840-1. PMID:29241458.
[21] Saisana M, Griffin SM, May FEB. Insulin and the insulin receptor collaborate to promote human gastric cancer. Gastric Cancer 2022;25(1):107–23. https://doi.org/10.1007/s10120-021-01236-y. PMID:34554347.
[22] Jeong I, Kang SK, Kwon WS, et al. Regulation of proliferation and invasion by the IGF signalling pathway in Epstein-Barr virus-positive gastric cancer. J Cell Mol Med 2018;22(12):5899–908. https://doi.org/10.1111/jcmm.13859. PMID:30247804.
[23] Zavros Y, Merchant JL. The immune microenvironment in gastric adenocarcinoma. Nat Rev Gastroenterol Hepatol 2022;19(7):451–67. https://doi.org/10.1038/s41575-022-00591-0. PMID:35288702.
[24] Joshi SS, Badgwell BD. Current treatment and recent progress in gastric cancer. CA Cancer J Clin 2021;71(3):264–79. https://doi.org/10.3322/caac.21657. PMID:33592120.
[25] Lei ZN, Teng QX, Tian Q, et al. Signaling pathways and therapeutic interventions in gastric cancer. Signal Transduct Target Ther 2022;7(1):358. https://doi.org/10.1038/s41392-022-01190-w. PMID:36209270.